Progress In Electromagnetics Research C, Vol. 12, 225–236, 2010

MICROSTRIP TRANSMISSION LINE LOADED BY SPLIT-RING RESONATORS TUNED BY FERROELECTRIC THIN FILM

G. Houzet, X. Mélique, and D. Lippens

IEMN-CNRS, DOME Group
University of Lille 1
Ave. Poincaré, Villeneuve d'Ascq Cedex 59652, France

L. Burgnies, G. Velu, and J.-C. Carru

LEMCEL
University of Littoral Côte d'Opale
Rue Ferdinand Buisson, Calais Cedex 62228, France

Abstract—The resonance frequency of Split-Ring Resonators (SRRs) loading a microstrip transmission line was tuned by means of a $Ba_{0.5}Sr_{0.5}TiO_3$ (BST) ferroelectric thin film. For a bias of 30 Volts, we obtained a band-stop response with a shift around 7% of the resonance to higher frequencies in K_u band. The originality of the device under test is (i) the utilisation of single C-shaped SRRs, (ii) the localisation via chemical etching of the BST film to voltage controlled interdigitated capacitances and (iii) the enhancement of the operating frequency (around 17 GHz).

1. INTRODUCTION

Ferroelectric thin films, and especially $BaSrTiO_3$ (BST), are currently attracting much interest for their integration in microwave tunable devices. Furthermore, metamaterials based technologies are now sufficiently mature to consider their tuneability [1–5]. Two fabrication approaches are currently investigated: The first one, which is relatively broad band, is based on Brillouin idea which consists to periodically load a transmission line by series capacitance and shunt inductance. The tuneability of such a configuration was recently demonstrated by using a ferroelectric technology [6] with notably the possibility to

Corresponding author: D. Lippens (didier.lippens@iemn.univ-lille1.fr).

tune the balance composite right-left handed dispersion characteristic of a Coplanar WaveGuide (CPW) transmission line [7]. The second approach takes benefit of Split-Ring Resonators (SRRs), which are narrow band in essence [8], and which exhibit an artificial magnetic dipole for a proper polarization of the incident magnetic field. Basically, a SRR can be described by a L-C equivalent circuit and thus the resonance frequency can be tuned by the capacitance value. So far, the tuneability, based on this principle, was demonstrated mainly by means of varactor diodes [9, 10] and recently by using uniform ferroelectric films [11] with a bias in excess of 140 Volts. In this paper, we address the possibility to tune the SRR frequency response with $Ba_{0.5}Sr_{0.5}TiO_3$ controlled by a dc electric field under moderate voltages. To this aim, we used a C-shaped geometry rather than the conventional edge-coupled SRR configuration [12] and interdigitated capacitances (IDC's) which were patterned on a micron scale onto a submicron-thick microstructured BST layer.

Basically, varactor diodes can be tuned with a low driving voltage and may exhibit a high aspect ratio between the zero-bias capacitance and the saturation one by a proper engineering of their doping profile. Commercial devices are thus available and was used so far for the tuning of split ring resonator and open ring resonator. Their frequency of operation, at least in their commercial version with surface mounted devices, is however rapidly limited by the active area and by the extrinsic element which dramatically reduce their pass band. For instance in the recent publication [13] the typical frequency of operation is 3 GHz whereas the present demonstration of a tuneable device by means of ferroelectric films was demonstrated at K_u band (12–18 GHz). In this paper, we address the possibility to tune the SRR frequency with $Ba_{0.5}Sr_{0.5}TiO_3$ controlled by a dc electric field under moderate voltage and to increase dramatically the operation frequency by taking advantage of the dielectric relaxation of BST films in the terahertz frequency range.

2. BST THIN FILM CHARACTERIZATION

A 260 nm thick $Ba_{0.5}Sr_{0.5}TiO_3$ (BST) ferroelectric thin film is deposited by a sol-gel process [14] on a 500 μm thick sapphire substrate. For electrical characterizations, IDC's were monolithically integrated onto this sapphire substrate as end-loads of CPW transmission lines, so that the propagation is monomode up to 110 GHz. The choice of a ratio of 0.5 in the composition of barium and strontium was motivated by the possibility to achieve a paraelectric phase, observed above the Curie temperature T_c, at room temperature avoiding by this means

hysterisis effects. It can be shown [15] that T_c is around 237 K this result being verified by an experimental investigation of the capacitance characteristics by taking the temperature as a parameter [16]. In addition, in order to de-embed the transmission line access in front the IDC, unloaded CPW transmission lines were also considered on the mask set [17]. The frequency dependence of the apparent capacitance of an IDC is plotted up to 110 GHz on Figure 1. As explained in reference [16], the term "apparent capacitance", de-embedded from the reflection coefficient in the IDC plane, was used because the finger inductance of IDC's (inset of Figure 1) plays an increasing role at millimeter waves. One can estimate their resonant frequency, with the varactor capacitance, in the 140–210 GHz band. As a consequence, while we expect a decrease of the permittivity value of BST films

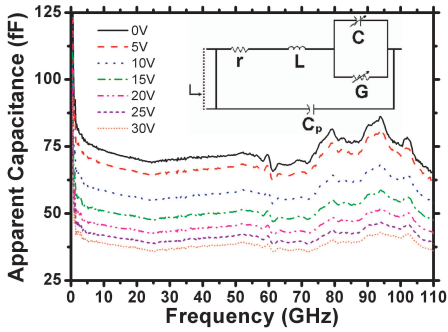

Figure 1. Frequency dependence of the apparent capacitance of an IDC measured up to 110 GHz at room temperature and taking the bias voltage as parameter. The inset shows the equivalent circuit of the IDC.

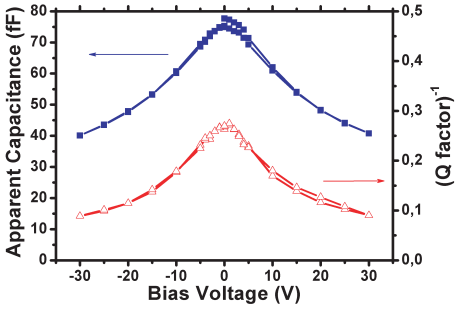

Figure 2. Capacitance (blue squares) and inverse Q factor (red triangles) measured at 100 GHz as a function of bias voltage.

and hence of the capacitance for a pure capacitance equivalent circuit at increasing frequency, the slight increase of the reactive term counterbalance the primary decrease due to the dispersion. Taking the bias voltage as a parameter it can be shown that the tuneability is almost constant over the very broad band investigated here from 0.4 GHz up to 110 GHz. Furthermore, it can be noticed that the frequency dependence of the capacitance value by varying the bias voltage between 0 and 30 V are quite similar. This shows that the tuneability of the device, which can be defined as the ratio of the zero bias capacitance and of the saturation capacitance, here around 30 V, is relatively constant versus frequency. Figure 2 shows the apparent capacitance and the loss tangent $(Q)^{-1}$ versus the tuning bias voltage recorded for a frequency of 100 GHz close to the upper frequency of the vectorial network analyser. In the present case, the IDC has a finger spacing of 1 µm. The tuneability is around 50% at 100 GHz for a maximal field of 300 kV/cm. Also, there is no hysteresis effect on the C(V) which indicates that the sample is in a paraelectric state at room temperature. As expected, the best quality factor is achieved under saturation condition.

3. DESIGN AND FABRICATION

The demonstration of the tuneability principle, outlined above, is here experimentally assessed via a microstrip transmission line loaded by two C-shaped micro-resonators as illustrated by the layout displayed in Figure 3(a). The coupling region between the microstrip line and the SRRs is carefully described in reference [18]. In a first stage, the square-shaped resonator dimensions (square side 940 µm, metal width

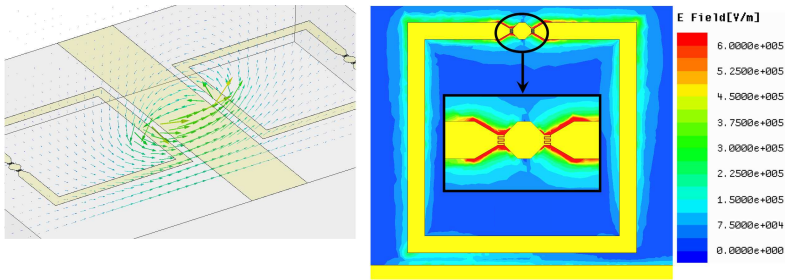

(a) (b)

Figure 3. (a) Circuit layout and illustration of the magnetic coupling and (b) magnitude of the electric field in the vicinity of IDCs.

70 µm) were determined by targeting a K_u operating band on the basis of our previous works on ferroelectric varactors [16] and the results on open ring resonators published in reference [19]. A simple formula permits one to estimate the inductance for ribbon inductors [20]:

$$L\,(\text{nH}) = 2l \times 10^{-4}\left[\ln\left(\frac{l}{w+t}\right) + 1.193 + \frac{w+t}{3l}\right] \times K_g \qquad (1)$$

with:

$$K_g = 0.57 - 0.145 \times \ln\left(\frac{w}{h}\right), \quad \frac{w}{h} > 0.05 \qquad (2)$$

The terms w, l, t and h, measured in µm, are respectively the width, the length, the metal thickness and substrate thickness of the inductor. In our case, with $w = 70$ µm, $l = 3460$ µm, $t = 0.55$ µm and $h = 500$ µm the inductance L has a value of 3.01 nH.

For the present device, each capacitance consists of five fingers with a width of 3 µm and a finger spacing of 1 µm. The length of each finger is 10.5 µm. The Figure 5(c) illustrates the technologies for the fabrication of varactors by a scanning electron micrograph (SEM) of a capacitance with a ferroelectric pad apparent underneath the fingers. By applying conformal mapping techniques on multilayered substrate [21], a capacitance value of around 40 fF was found. As the two interdigitated capacitances (IDCs) are in a series configuration, the equivalent capacitance value C is 20 fF. The resonant frequency F_0 of the SRR can be estimated by considering an equivalent L-C circuit which the resonance frequency is given by:

$$F_0 = \frac{1}{2\pi\sqrt{LC}} \qquad (3)$$

with the values of L and C calculated previously, F_0 is estimated to around 20 GHz. However, mutual inductances phenomena increase the value of L calculated, and results to a slight decrease of F_0.

In a second stage, full wave analysis of the two-port circuit was carried out in order to optimize the magnetic coupling which is required for the achievement of a magnetic dipole. Both stages were conducted by means of the commercial software HFSS by Ansoft. The magnetic coupling is illustrated by the plotting of $\vec{H}$ field in Figure 3(a) in a plane transverse to the propagation direction at the SRR location. It can be noticed that the wrapping of the magnetic field around the central strip of the microstrip line permits one to induce current loops in the side resonators. An electric field map in the resonator plane, along a zoomed view in the vicinity of voltage controlled varactors, is shown in Figure 3(b). We used interdigitated capacitances on a microscale. Under this condition, the local electric field value is high even for a

moderate controlling voltage so that significant changes in the BST permittivity, with subsequent capacitance variations, can be achieved. The ground resonance mode of the ring is observed by plotting the current distributions at the resonance of the SRR on the Figure 4. The lack of node on this vectorial representation indicates that we excite the first resonance mode.

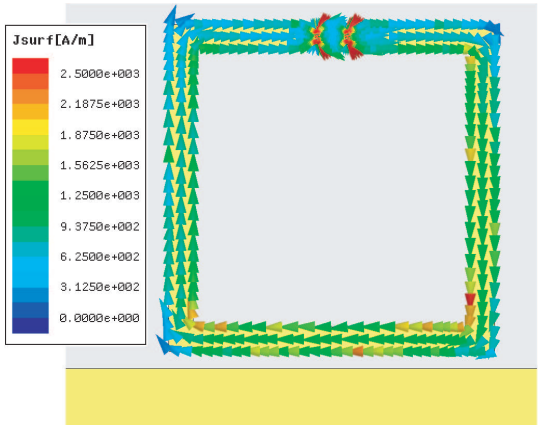

Figure 4. Surface currents plotted at the resonant frequency of the ring.

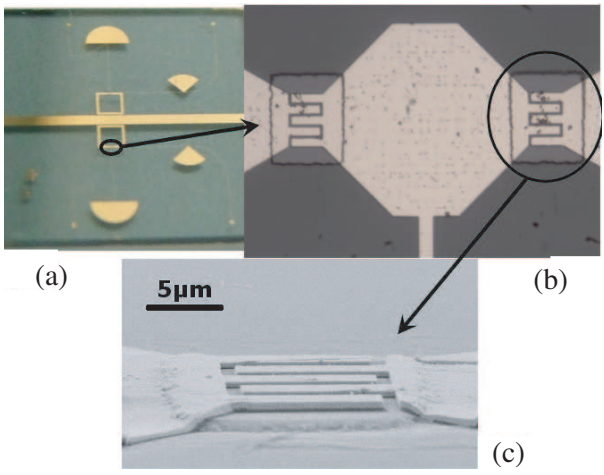

Figure 5. (a) Microstrip transmission line loaded by two SRRs and its bias circuit. (b) Optical view of two tunables IDCs and (c) SEM of an IDC.

Figure 5 illustrates the technological stages which were used for the fabrication of circuit. The first stage was the deposition of a 260 nm-thick BST film by a sol gel technique [14] onto a 500 µm-thick sapphire substrate. Owing to the localization of the electric field component exemplified above (Figure 3(b)), it was also decided to selectively etch the BST layer (Hexa-Fluoride HF etching) prior to the IDC patterning by electron beam lithography (LEICA EBPG 5000-Plus) and subsequent metal deposition by gold evaporation (Meca 2000). Furthermore in order to avoid a short circuit via the resonator stripline, the dc bias was supplied at the central point of two IDC's as shown in Figure 5(b). The bias circuit uses half- and quarter-moon stubs and $\lambda_g/4$ ultra narrow lines. Those stubs bring a short circuit at a specific frequency in the plane where they are located. In our case, the operating frequency is chosen as the ground resonant mode of the SRRs. By employing $\lambda_g/4$ lines, the short circuit is transformed in an open circuit. The impedance dispersion of the stubs can be calculated following Eq. (4) [22]:

$$Z_{in} = -jZ_0\left(r_{ie}\right)\cot\left(kr_{ie}, kr_{oe}\right) \tag{4}$$

with:

$$\cot\left(kr_{ie}, kr_{oe}\right) = \frac{N_0\left(kr_{ie}\right)J_1\left(kr_{oe}\right) - J_0\left(kr_{ie}\right)N_1\left(kr_{oe}\right)}{J_1\left(kr_{ie}\right)N_1\left(kr_{oe}\right) - N_1\left(kr_{ie}\right)J_1\left(kr_{oe}\right)} \tag{5}$$

$$Z_0\left(r_{ie}\right) = \frac{120\pi h}{r_{ie}\Phi\sqrt{\epsilon_r}} \tag{6}$$

where J_i and N_i are the Bessel and Neumann functions of ith order. k is the wave number, h the thickness of the substrate (500 µm in our case), Φ the aperture angle of the stub (90° (quarter moon)or 180° (half moon) in our case), r_{oe} the radius of the stub (800 µm), $r_{ie} = W_g/(2 \times \sin\{\Phi/2\})$ with W_g the connection's width between the stub and the line (5 µm).

4. RESULTS AND INTERPRETATION

The scattering parameters of the filter were measured by means of a vectorial analyzer (Agilent 8510C XF), after assembling the circuit, fabricated on the sapphire substrate, with a dc bias printed circuit board and subsequent wire bonding. Then the overall circuit was mounted in a commercial test fixture (Anritsu 3680V). The measurements were performed at room temperature where the ferroelectric is in a paraelectric phase, as seen before, for the 50% Barium concentration considered here, so that hysteresis effects have been avoided. The voltage was varied between 0 and 30 Volts with

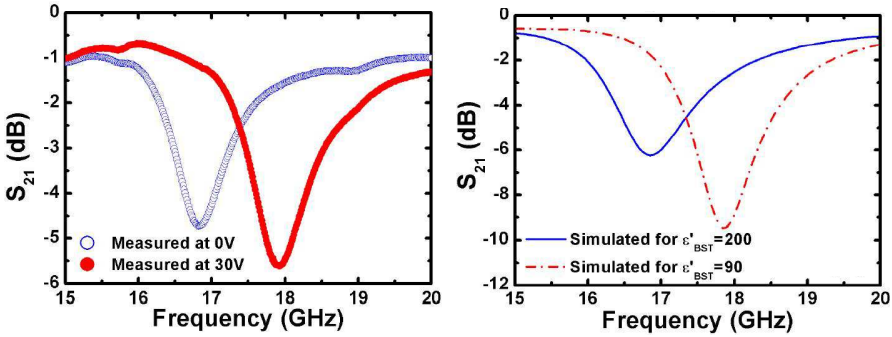

Figure 6. Comparison of S_{21} parameters versus frequency for (a) measurements and (b) full-wave simulations.

an expected tuneability of the capacitance around 50% (Figure 2). This high tuneability can be explained by the large variations of the AC electric field in the vicinity of the varactors which reaches values in excess of 100 kV/cm for moderate voltage (few tens volts for micron scales interdigitated devices). Figure 6(a) shows the frequency dependence of the magnitude of the scattering parameter S_{21} which was measured experimentally between 15 and 20 GHz for an unbiased and biased (30 Volts) device. As expected the device exhibits a band-stop filtering characteristic with a relevant frequency around 17 GHz for unbiased devices. Beyond the circuit consideration, it can be shown that the rejection, pointed out here, is due to the achievement of a negative permeability above the resonance frequency of microresonators while the effective permittivity is still positive. In the frequency range between the resonance frequency and the so-called plasma frequencies, the structures can be considered as a single magnetic medium with a zero-transmission. Due to the fact that we loaded the transmission line by solely two SRR's, facing each other, the rejection level is around -5 dB. However, this level can be dramatically improved by cascading periodically more cells in the propagation direction. By applying a dc bias of 30 Volts, a shift towards higher frequencies can be noted with a slight improvement in the notch depth which results from a known improvement of the quality factor of BST films under bias. The corresponding tuneability is around 7% for a bias voltage variation of 30 Volts. Comparable tuneability values (12%) was recently published in the literature [11] with rejection level of the same order of magnitude. However, it should be noticed that the bias voltage was 140 Volts for this reference and hence four times

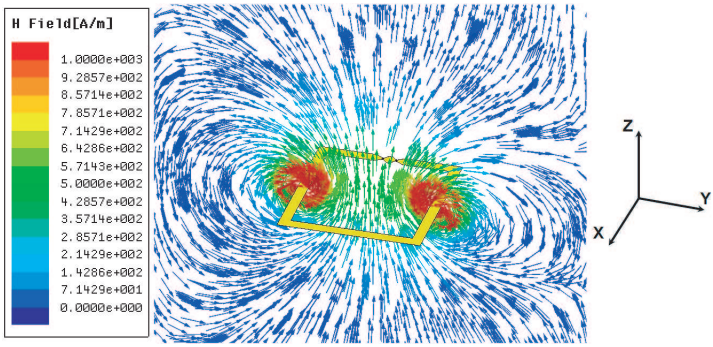

Figure 7. Illustration of the magnetic dipole by the vectorial plotting of the magnetic field in a normal plane of a SRR in free space at its resonant frequency. The vector magnetic field is shown in the z-y plane through the middle of the cell.

higher that the controlling voltage of the present work. Figure 6(b) shows the frequency variation of S_{21} which was calculated by full wave simulations by varying the input data of the BST permittivity ($\epsilon_r = 200$ for zero-bias and $\epsilon_r = 90$ at saturation). A satisfactory agreement was obtained in the description of the frequency shift while the trends in the rejection are also reproduced numerically.

From a physical point of view, this device shows the possibility to control a magnetic dipole by an electrical one. Indeed, the magnetic dipole is illustrated in Figure 7, on which we plotted the contour of the magnetic field vectors at the resonant frequency of a SRR in free space. The mapping is comparable to the one of a permanent magnet. Concerning the electric dipole, it can be identified as the ferroelectric thin film which can be electrically controlled by a bias voltage.

It can be shown that the dispersion of the real part of the effective permeability versus frequency follows a Lorentz-type law with two relevant frequencies, the resonance and the magnetic plasma respectivelly. By tuning the value of the BST permittivity, capacitance decreases and varies the resonance frequency towards higher frequency (blue shift). The magnetic plasma frequency is related to the resonance frequency via the filling factor. As a consequence, the overall frequency band where the propagation medium is single negative through the permeability is shifted to higher frequencies.

5. CONCLUSION

A tuneable band-stop filter in a microstrip Split Ring Resonator technology has been fabricated and characterized at K_u band. A tuneability around 7% of the central frequency was demonstrated experimentally under a moderate control voltage of 30 Volts. Further improvements could be expected (i) for the rejection level by periodically loading the transmission line, (ii) in the voltage control by further shrinking the finger spacing of IDCs and (iii) of the tuneability by thicker BST epilayers.

ACKNOWLEDGMENT

The authors would like to thank D. Troadec, F. Vaurette, D. Vandermoere, D. Szymik, K. Blary for their help in the fabrication and V. Avramovic for her help in the characterization.

REFERENCES

1. Wu, B. I., W. Wang, J. Pacheco, X. Chen, T. Grzegorczyk, and J. A. Kong, "A study of using metamaterials as antenna substrate to enhance gain," *Progress In Electromagnetics Research*, PIER 51, 295–328, 2005.
2. Monti, G. and L. Tarricone, "Negative group velocity in a split ring resonator-coupled microstrip line," *Progress In Electromagnetics Research*, PIER 94, 33–47, 2009.
3. Wang, J., S. Qu, J. Zhang, H. Ma, Y. Yang, C. Gu, X. Wu, and Z. Xu, "A tunable left-handed metamaterial based on modified broadside-coupled split-ring resonators," *Progress In Electromagnetics Research Letters*, Vol. 6, 35–45, 2009.
4. Chen, J. Y., W. L. Chen, J. Y. Yeh, L. W. Chen, and C. C. Wang, "Comparative analysis of split-ring resonators for tunable negative permeability metamaterials based on anisotropic dielectric substrates," *Progress In Electromagnetics Research M*, Vol. 10, 25–38, 2009.
5. Hand, T. H. and S. A. Cummer, "Frequency tunable electromagnetic metamaterial using ferroelectric loaded split rings," *J. Appl. Phys.*, Vol. 103, 066105, 2008.
6. Kuylenstierna, D., A. Vorobiev, P. Linnér, and S. Gevorgian, "Composite right/left handed transmission line phase shifter using ferroelectric varactors," *IEEE Microw. and Wireless Comp. Lett.*, Vol. 16, No. 4, 167–169, 2006.

7. Marteau, A., G. Velu, G. Houzet, L. Burgnies, E. Lheurette, J.-C. Carru, and D. Lippens, "Ferroelectric tunable balanced right- and left-handed transmission lines," *Appl. Phys. Lett.*, Vol. 94, 023507, 2009.
8. Pendry, J. B., A. J. Holden, D. J. Robbins, and W. J. Stewart, "Magnetism from conductors and enhanced nonlinear phenomena," *IEEE Trans. on Microw. Theory and Tech.*, Vol. 47, No. 11, 2075–2084, 1999.
9. Gil, I., J. Garcia-Garcia, J. Bonache, F. Martin, M. Sorolla, and R. Marques, "Varactor-loaded split ring resonators for tunable notch filters at microwave frequencies," *Electron. Lett.*, Vol. 40, No. 21, 1347–1348, 2004.
10. Shadrivov, I. V., S. K. Morrison, and Y. S. Kivshar, "Tunable split-ring resonators for non-linear negative index metamaterials," *Opt. Expr.*, Vol. 14, No. 20, 9344–9349, 2006.
11. Gil, I., C. Damn, A. Giere, M. Sazegar, J. Bonache, R. Jakoby, and F. Martin, "Electrically tunable split-ring resonators at microwave frequencies based on barium-strontium-titanate thick films," *Electron. Lett.*, Vol. 45, No. 8, 417–418, 2009.
12. Ekmekci, E. and G. Turhan-Sayan, "Comparative investigation of resonance characteristics and electrical size of the double-sided SRR, BC SRR and conventional SRR type metamaterials for varying substrate parameters," *Progress In Electromagnetics Research B*, Vol. 12, 35–62, 2009.
13. Shadrivov, I. V., A. B. Kozyrev, D. W. van der Weide, and Y. S. Kivshar, "Tunable transmission and harmonic generation in nonlinear metamaterials," *Appl. Phys. Lett.*, Vol. 93, 161903, 2008.
14. Velu, G., J.-C. Carru, E. Cattan, D. Remiens, X. Melique, and D. Lippens, "Deposition of ferroelectric BST thin films by sol gel route in view of electronic applications," *Ferroelectrics*, Vol. 288, 59–69, 2003.
15. Vendik, O. G., S. P. Zubko, and M. A. Nikol'ski, "Microwave loss factor of $BaSrTiO_3$ as a function of temperature, biasing field, barium concentration, and frequency," *J. Appl. Phys.*, Vol. 92, 7448–7452, 2002.
16. Houzet, G., L. Burgnies, G. Velu, J.-C. Carru, and D. Lippens, "Dispersion and loss of ferroelectric $Ba_{0.5}Sr_{0.5}TiO_3$ thin films up to 110 GHz," *Appl. Phys. Lett.*, Vol. 93, 053507, 2008.
17. Burgnies, L., G. Velu, G. Houzet, K. Blary, J.-C. Carru, and D. Lippens, "A TRL-like calibration for tunable interdigitated BST varactors," *IEEE Trans. on Instr. and Meas.*, Vol. 57, No. 6,

1127–1132, 2008.

18. Mao, S.-G. and S.-L. Chen, "Characterization and modeling of left-handed microstrip lines with application to loop antennas," *IEEE Trans. on Antennas and Prop.*, Vol. 54, No. 4, 1084–1091, 2006.
19. Rogla, L. J., J. Carbonell, and V. E. Boria, "Study of equivalent circuits for open-ring and split-ring resonators in coplanar waveguide technology," *IET Microw. Antennas Propag.*, Vol. 1, 170–176, 2007.
20. Bahl, I. J., *Lumped Elements for RF and Microwave Circuits*, Artech House, 2003.
21. Gevorgian, S. S., T. Martinsson, P. L. J. Linnér, and E. L. Kollberg, "CAD models for multilayered substrate interdigital capacitors," *IEEE Trans. on Microw. Theory and Tech.*, Vol. 44, No. 6, 896–904, 1996.
22. Sorrentino, R. and L. Roselli, "A new simple and accurate formula for microstrip radial stub," *IEEE Microw. and Guided Waves Lett.*, Vol. 2, No. 12, 480–482, 1992.